Articles

Synthesis, Stereochemical Identification, and Selective Inhibitory Activity against Human Monoamine Oxidase-B of 2-Methylcyclohexylidene-(4-arylthiazol-2-yl)hydrazones

Franco Chimenti,[†] Elias Maccioni,[‡] Daniela Secci,*[,†] Adriana Bolasco,[†] Paola Chimenti,[†] Arianna Granese,[†] Simone Carradori,[†] Stefano Alcaro,[§] Francesco Ortuso,[§] Matilde Yáñez,[||] Francisco Orallo,[||] Roberto Cirilli,[⊥] Rosella Ferretti,[⊥] and Francesco La Torre[⊥]

Dipartimento di Studi di Chimica e Tecnologia delle Sostanze Biologicamente Attive, Università degli Studi di Roma "La Sapienza", P.le A. Moro 5, 00185 Roma, Italy, Dipartimento Farmaco Chimico Tecnologico, Università degli Studi di Cagliari, Via Ospedale 72, 09124 Cagliari, Italy, Dipartimento di Scienze Farmaco Biologiche "Complesso Ninì Barbieri", Università degli Studi di Catanzaro "Magna Graecia", 88021 Roccelletta di Borgia (CZ), Italy, Departamento de Farmacología, Facultad de Farmacia, Universidad de Santiago de Compostela, Campus Universitario Sur, E-15782 Santiago de Compostela (La Coruña), Spain, and Dipartimento del Farmaco, Istituto Superiore di Sanità, V.le Regina Elena 299, 00161 Roma, Italy

Received February 7, 2008

A series of 2-methylcyclohexylidene-(4-arylthiazol-2-yl)hydrazones have been investigated for their ability to inhibit selectively the activity of the human A and B isoforms of monoamine oxidase (MAO). The target compounds, which present a stereogenic center on the cyclohexane ring, were obtained as pure (*R*) and (*S*) enantiomers by enantioselective HPLC. The absolute configuration of homochiral forms isolated on a semipreparative scale was obtained by a combined strategy based on chemical correlation and single-crystal X-ray diffraction. All compounds showed higher activity against the human MAO-B isoform with IC_{50} values ranging between 26.81 ± 2.74 μM and 14.20 ± 0.26 nM, and the assays carried out on the pure enantiomers showed higher activity for the (*R*) form. A computational study was performed by molecular mechanics, DFT-based quantomechanics, and docking techniques on the most active and human MAO-B selective inhibitor **8**.

Introduction

Monoamine oxidases (MAOs[a]) are flavin adenine dinucleotide (FAD) containing enzymes present in the outer mitochondrial membranes of neuronal, glial, and other cells. They catalyze the oxidation of endogenous and exogenous amines to the corresponding aldehyde while releasing H_2O_2 and ammonia.[1] MAOs exist in two forms, namely, MAO-A and MAO-B, encoded by separate genes sharing a common intron/exon organization.[1–3] The two MAO isoforms have been identified according to their substrate specificity and selective inhibitors. The typical MAO-A substrate is 5-hydroxytryptamine (5-HT), while 2-phenylethylamine (PEA) and benzylamine are MAO-B substrates.[4] Clorgyline and moclobemide are two selective reference inhibitors for MAO-A, while *R*-(−)-deprenyl (selegiline), rasagiline, and lazabemide are well-known selective inhibitors of MAO-B (Figure 1).[5,6]

Since they metabolize the principal biogenic amines, MAO-A and MAO-B play an important role in the regulation of their concentrations mainly in the central nervous system, where abnormal values have been involved in psychiatric and neurodegenerative disorders such as Alzheimer's disease (AD) and Parkinson's disease (PD).[7,8] Therefore, selective and reversible inhibitors of MAO-A or MAO-B may be useful therapeutic agents devoid of unwanted side effects such as the so-called "cheese effect".[9]

In humans MAO-B inhibitors are useful in the treatment of PD and AD,[10–13] while MAO-A inhibitors are antidepressant and antianxiety agents (Figure 1).[14,15]

The recent description of the crystal structure of the two isoforms of human MAO (hMAO) by Binda et al. has provided relevant information about the recognition mechanism underlying the selective interactions between these proteins and their ligands, in order to probe the catalytic mechanism and gain a better understanding of the pharmacophoric requirements needed for the rational design of potent and selective enzyme inhibitors with therapeutic potential.[16–20]

In the course of our research we have previously reported the synthesis and inhibitory activity of a series of selective 2-thiazolylhydrazone MAO-B inhibitors,[21] and as part of our plan in this work, we study the inhibitory activity of 2-methylcyclohexylidene-(4-arylthiazol-2-yl)hydrazones on hMAO-A

* To whom correspondence should be addressed. Phone: +39 06 4991 3763. Fax: +39 06 49913772. E-mail: daniela.secci@uniroma1.it.
[†] Università degli Studi di Roma "La Sapienza".
[‡] Università degli Studi di Cagliari.
[§] Università degli Studi di Catanzaro "Magna Graecia".
[||] Universidad de Santiago de Compostela.
[⊥] Istituto Superiore di Sanità.

[a] Abbreviations: MAO, monoamine oxidase; FAD, flavin adenine dinucleotide; 5-HT (5-hydroxytryptamine); PEA, 2-phenylethylamine; AD, Alzheimer's disease; PD, Parkinson's disease; IC_{50}, 50% inhibition constant; HPLC, high-performance liquid chromatography; CPSs, polysaccharide-based chiral stationary phases; DFT-based, density functional theory; MC, Monte Carlo; MM, molecular mechanics; MMFF, molecular mechanics force field; QM, quantum mechanic; GB/SA, Gibbs Born/surface area; 2-MCE, 2-methylcyclohexanone; 2-MCET, 2-methylcyclohexylidene-thiosemicarbazone; K_m, Michaelis constant; V_{max}, maximum reaction velocity; BTI-TN-5B1-4, insect cells infected with recombinant baculovirus containing cDNA; PDB, Protein Data Bank; 2BXR, PDB code of hMAO-A; 1GOS, PDB code of hMAO-B; SEM, standard error of the mean; *P*, probability value; $pIC_{50} = -\log IC_{50}$. Abbreviations used for amino acids follow the rules of the IUPACIUB Commission of Biochemical Nomenclature in *J. Biol. Chem.* **1972**, *247*, 977−983. Amino acid symbols denote L-configuration unless otherwise indicated.

10.1021/jm800132g CCC: $40.75
Published on Web 07/31/2008

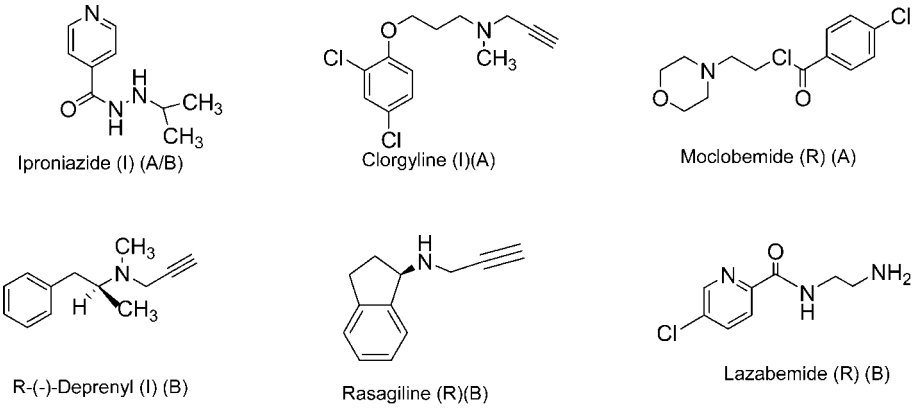

Figure 1. Irreversible (I), reversible (R), and selective MAO-A and/or MAO-B (A or A/B or B) inhibitors.

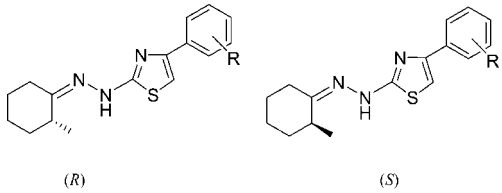

Figure 2. (*R*)- and (*S*)-Enantiomers of the 2-methylcyclohexylidene-(4-arylthiazol-2-yl)hydrazones derivatives (**1**−**9**).

Scheme 1. Synthesis of Compounds **1**−**9**[a]

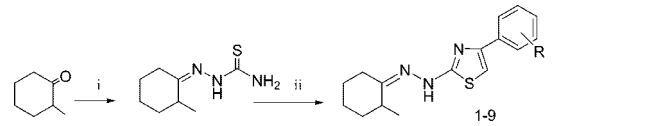

[a] Reagents and conditions: (i) thiosemicarbazide, 2-propanol, acetic acid; (ii) α-halogenoketone, 2-propanol, room temp.

and hMAO-B. Owing to the presence of a stereogenic carbon on the cyclohexyl ring, these compounds exist as (*R*)- and (*S*)-enantiomers (Figure 2).

The first step toward the investigation of the impact of absolute stereochemistry on the activity and selectivity was to isolate sufficient quantities of the enantiomers of four of the most active compounds to use in a parallel test in vitro. Our strategy was to synthesize the racemic forms and successively resolve them by HPLC on polysaccharide-based chiral stationary phases (CPSs) on a semipreparative scale. A combined method based on chemical correlation, single-crystal X-ray diffraction, and enantioselective HPLC allowed us to assign the absolute configuration of the isolated enantiomers.

Knowledge of the absolute configuration and in vitro biological activity of homochiral forms was needed in the in silico study of the interactions involving the receptor site.

In this paper we present the synthesis, the enantioseparation of the 2-methylcyclohexylidene-(4-arylthiazol-2-yl)hydrazones (**1**−**9**), the stereoselective synthesis of the pure enantiomers, and the absolute configuration. We also report their inhibitory activity against the A- and B-isoforms of hMAO, a computational approach for the study of the conformational properties of the molecules, and the docking of the most active and selective compound **8**, using the crystal structure data and models of the hMAO-A and hMAO-B, deposited in the Protein Data Bank.

Chemistry

Racemic 2-thiazolylhydrazone derivatives (**1**−**9**) were synthesized as reported in previous communications by us[22,23] (Scheme 1). 2-Methylcyclohexanone (2-MCE) reacted directly with thiosemicarbazide, and the obtained 2-methylcyclohexylidene-thiosemicarbazone (2-MCET) subsequently reacted with α-halogenoketones to yield the 4-substituted thiazole derivatives. In the synthesis of all compounds, 2-propanol proved to be the best solvent for our purpose. As a matter of fact, the reaction products precipitate and can be filtered and purified by crystallization from ethanol or ethanol/isopropanol. All the synthesized

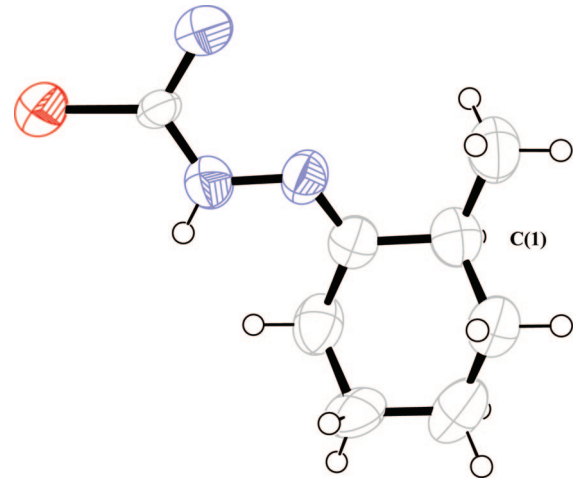

Figure 3. X-ray structure of (+)-(*S*)-2-MCET.

products were characterized by spectroscopic methods (see Supporting Information).

For the stereocontrolled synthesis of the pure enantiomers of compounds **3**, **5**, **8**, and **9**, we use the enantiopure forms of 2-MCET as chiral synthon on the basis of a previous study by us on the enantioseparation and configurational stability of this compound.[24] The racemic 2-MCET obtained in the first step of the reaction was separated by enantioselective HPLC on a semipreparative scale, and the isolated pure enantiomers were used for the second step.

The absolute configuration of the chiral synthon was established by a single crystal X-ray diffraction analysis. The molecular structure is illustrated in Figure 3. From the findings of the X-ray structure analysis, we can assign unambiguously the (*S*)-configuration to the C2 stereogenic center located on the cyclohexyl ring (labeled C(1) in Figure 3) of the (+)-2-MCET enantiomer.

Starting from the enantiopure forms of 2-MCET of known stereochemistry, we obtained enantioenriched forms of the target

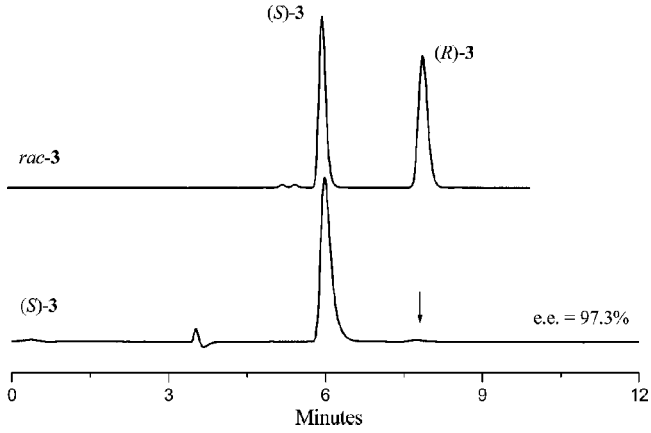

Figure 4. Check of the stereochemical course of the synthesis of (*S*)-**3** starting from (*S*)-**2**-MCET: column, Chiralpak AS-H (250 mm × 4.6 mm i.d.); eluent, methanol; flow rate, 1 mL/min; temperature, 25 °C; detection, UV at 310 nm.

molecules with correlated chirality. The stereochemical course of the reaction was monitored by the same enantioselective HPLC system used for the semipreparative enantioseparation. The cyclization of the chiral synthon is stereoconservative as demonstrated by the high ee values (95−98%) of the obtained thiazoles.

As an example, in Figure 4 we report the chromatograms relating to the control of the enantiomeric purity of (*S*)-**3** and the enantiomeric elution order assignment of its racemic form.

The assignment of the absolute configuration of the enantiomers of compounds **1**−**9** was determined by chemical correlation using as reference compound the chiral synthon 2-MCET.[24]

Results and Discussion

Thiazoles **1**−**9** were synthesized at the beginning as racemates and evaluated for their ability to inhibit the A and B isoforms. The test drugs (new compounds and reference inhibitors) themselves do not directly react with the Amplex Red reagent, which indicates that these drugs do not interfere with the measurements. In our experiments and our experimental conditions, hMAO-A displayed a Michaelis constant (K_m) of 457.17 ± 38.62 μM and a maximum reaction velocity (V_{max}) of 185.67 ± 12.06 (nanomol/min)/mg protein whereas hMAO-B showed a K_m of 220.33 ± 32.80 μM and a V_{max} of 24.32 ± 1.97 (nanomol/min)/mg protein (n = 5). The tested drugs (new compounds and reference inhibitors) inhibited these control enzymatic MAO activities, and the inhibition was concentration dependent.

As shown in Table 1, the new compounds were significantly selective hMAO-B inhibitors. For this reason it was important to have the pure enantiomers of the most active compounds in order to evaluate the influence of stereochemistry on the inhibitory activity. With this in mind we performed a chromatographic separation of the enantiomers.

The HPLC enantioseparation was carried out on the amylose-based Chiralpak AD and Chiralpak AS-H CSPs using normal-phase and polar organic conditions (for details, see the Supporting Information). The absolute configuration of the isolated homochiral forms on semipreparative level was assigned by comparing their elution order with that of the enantiomers of known stereochemistry obtained by stereoselective synthesis.

The choice to use 2-MCET instead of 2-MCE as a chiral synthon was based on the high configurational stability and better availability of the pure enantiomers of the former, as previously reported in a recent work by us.[24]

Table 1. Structures and Inhibitory Activities of Derivatives **1**−**9** and Reference Compounds

compd	R	IC_{50} [a] hMAO-A	IC_{50} [a] hMAO-B	ratio
1	H	41.23 ± 3.96 μM[b]	711.23 ± 36.95 nM	58
2	4-Cl	35.22 ± 1.81 μM[b]	13.12 ± 0.51 μM	2.7
3	4-F	43.55 ± 3.61 μM[b]	203.83 ± 8.52 nM	214
4	2,4-Cl	44.70 ± 5.23 μM[b]	26.81 ± 2.74 μM	1.7
5	2,4-F	37.95 ± 3.41 μM[b]	14.20 ± 0.26 nM	2,673
6	4-CH_3	*d*	142.64 ± 8.65 nM	>701[e]
7	4-OCH_3	2.76 ± 0.17 μM[b]	2.37 ± 0.14 μM	1.2
8	4-NO_2	*d*	32.33 ± 2.22 nM	>3093[e]
9	4-CN	31.03 ± 2.44 μM[b]	26.23 ± 1.02 nM	1,183
clorgyline		4.46 ± 0.32 nM[b]	61.35 ± 1.13 μM	0.000073
R-(−)-deprenyl		67.25 ± 1.02 μM[b]	19.60 ± 0.86 nM	3431
iproniazide		6.56 ± 0.76 μM	7.54 ± 0.36 μM	0.87
moclobemide		361.38 ± 19.37 μM	*c*	<0.36[f]

[a] Each IC_{50} value is the mean ± SEM from five experiments (n = 5). [b] Level of statistical significance: $P < 0.01$ versus the corresponding IC_{50} values obtained against MAO-B, as determined by ANOVA/Dunnett's test. [c] Inactive at 1 mM (highest concentration tested). [d] Inactive at 100 μM (highest concentration tested). At higher concentrations the compounds precipitate. [e] Values obtained under the assumption that the corresponding IC_{50} against hMAO-A is the highest concentration tested (100 μM). [f] Value obtained under the assumption that the corresponding IC_{50} against hMAO-B is the highest concentration tested (1 mM).

Table 2. Structures and Inhibitory Activities of Separated Enantiomers of Compounds **3**, **5**, **8**, and **9**

compd	R	IC_{50} [a] hMAO-A (μM)	IC_{50} [a] hMAO-B (nM)	ratio	ee (%)
(*S*)-**3**	4-F	4.94 ± 0.09[b]	47.24 ± 2.49	105	>99
(*R*)-**3**		3.53 ± 0.12[b]	22.01 ± 1.32	160	>95
(*S*)-**5**	2,4-F	4.81 ± 0.03[b]	36.06 ± 3.45	133	>99
(*R*)-**5**		6.83 ± 0.14[b]	30.08 ± 2.71	227	95
(*S*)-**8**	4-NO_2	42.31 ± 2.81[b]	16.58 ± 0.86	2552	>99
(*R*)-**8**		43.95 ± 1.08[b]	9.80 ± 0.67	4485	>99
(*S*)-**9**	4-CN	7.22 ± 0.56[b]	63.02 ± 3.62	115	>99
(*R*)-**9**		5.50 ± 0.26[b]	32.48 ± 2.25	169	>99

[a] Each IC_{50} value is the mean ± SEM from five experiments (n = 5). [b] Level of statistical significance: $P < 0.01$ versus the corresponding IC_{50} values obtained against hMAO-B, as determined by ANOVA/Dunnett's test.

In Table 1 we report the inhibitory activity of racemic compounds **1**−**9** against hMAO-A and hMAO-B, while Table 2 shows the activities of the pure enantiomers of compounds **3**, **5** (the most active), **8** (the most selective), and **9**, selected among all the racemic compounds for the next experiments.

From the results reported in Table 2 we can point out that the (*R*)-enantiomers are the most active and B-selective with hMAO-B IC_{50} values ranging between 32.48 ± 2.25 and 9.80 ± 0.67 nM and hMAO-B selectivity ratios ranging between 160 and 4485. Just to clarify, the results obtained in this work for the racemic mixture of compound **1**, 2-methylcyclohexylidene-(4-arylthiazol-2-yl)hydrazone partially disagree with the results previously published for the same compound.[21] This discrepancy may be due, at least in part, to the different methods and experimental conditions used in both studies. Compound (*R*)-**8**, with the best hMAO-B activity and B-selectivity, was therefore selected for the subsequent computational study.

In the reversibility and irreversibility tests, hMAO-A and hMAO-B inhibition was irreversible in presence of the racemic mixture and the enantiomers of compound **8** as shown by the lack enzyme activity restoration after repeated washing (Table 3). Similar results were obtained for the racemic mixture and the enantiomers of compound **5** against hMAO-A and hMAO-B (data not shown) and for *R*-(−)-deprenyl against hMAO-B (Table 3). However, significant recovery of hMAO-A activity

Table 3. Reversibility and Irreversibility of MAO Inhibition[a]

compd	hMAO-A inhibition (%) before washing	hMAO-A inhibition (%) after repeated washing
moclobemide (500 μM)	86.75 ± 4.34	10.26 ± 0.65[b]
8 (100 μM)	23.41 ± 1.62	26.61 ± 1.54
(*S*)-**8** (100 μM)	69.47 ± 3.76	71.47 ± 3.47
(*R*)-**8** (100 μM)	60.56 ± 2.98	58.43 ± 2.76

compd	hMAO-B inhibition (%) before washing	hMAO-B inhibition (%) after repeated washing
R-(−)-deprenyl (20 nM)	48.67 ± 2.34	49.14 ± 2.80
8 (50 nM)	58.65 ± 2.97	60.19 ± 3.26
(*S*)-**8** (50 nM)	74.32 ± 4.14	79.26 ± 4.32
(*R*)-**8** (50 nM)	77.83 ± 3.89	81.63 ± 4.25

[a] Each value is the mean ± SEM from five experiments ($n = 5$). [b] Level of statistical significance: $P < 0.01$ versus the corresponding % hMAO-A inhibition before washing as determined by ANOVA/Dunnett's test.

Table 4. Thermodynamic Docking Results of **8**·hMAO Complexes and Comparison with Experimental Inhibition Data

enzyme	C*	C=N	$\Delta\Delta E_{int}$ [a]	pIC_{50} [c]
hMAO-A	*R*	*E*	−40.58[b]	4.36
		Z	−33.53	
	S	*E*	−41.03[b]	4.37
		Z	−36.77	
hMAO-B	*R*	*E*	−42.32	8.00
		Z	−46.84[b]	
	S	*E*	−43.78[b]	7.78
		Z	−42.25	

[a] In kcal/mol. [b] ΔΔ interaction energy minimum. [c] $pIC_{50} = -\log IC_{50}$.

was observed after repeated washing of moclobemide, indicating that this drug is a reversible inhibitor of hMAO-A.

This selection of compound **8** was carried out following a similar approach reported in our previous communication.[21] For the presence in **8** of the asymmetric methylcyclohexylidene moiety and the thiosemicarbazone imine N=C double bond, we have modeled the *E* and *Z* isomers separately and kept the *R* configuration fixed by Monte Carlo (MC) simulations and the molecular mechanics force field (MMFF). The conformational distribution in the energies window within 12.5 kcal/mol above the global minimum structure was larger for the (*R*)-*E* than for the (*R*)-*Z* stereoisomer, with 59 and 40 unique conformers, respectively. The most stable conformers were then compared by a quantum mechanic (QM) method, as described in the Experimental Section. The MM and QM energy evaluation of the global (*R*)-*E* and (*R*)-*Z* minimum conformers of **8** revealed differences in stability, which were lower than 0.25 and 0.35 kcal/mol when measured in different solvating environments. Therefore, for compound **8**, in agreement with previous observations by us on other thiazole derivatives,[21] both stereoisomers can exist in physiological conditions and can contribute almost equally to the binding properties within the hMAO isoforms.

After converting the conformers of the *R* into the *S* enantiomer in both *E* and *Z* configurations, we used the four **8** ensembles to perform docking experiments on the hMAO pretreated enzyme models as described in the Experimental Section. First, in the rigid docking we included all the conformers obtained in the MC search. Then we fully energy-minimized the configurations of the eight possible combinations of hMAO isoforms and ligand stereoisomer. The thermodynamic interaction results are reported in Table 4.

Assuming that the enzyme inhibition is a function of the interaction energy, from a comparison with pIC_{50} a good correlation between theoretical and experimental data was observed. The trend can be highlighted, especially considering the lowest value of the *E* and *Z* configuration interaction energies for each of the eight complex ensembles. In three of the four complexes, that is, [(*R*)-**8**·hMAO-A], [(*S*)-**8**·hMAO-A], and [(*S*)-**8**·hMAO-B], the *E* configuration was ranked as the most stable of **8** for recognition within the enzymes. Conversely, the [(*R*)-**8**·MAO-B] complex was consistently stable when the *Z* configuration is adopted. In order to understand the thermodynamic results at the molecular level, we analyzed the four most stable complexes. In this analysis we considered the number of contacts and intermolecular hydrogen bonds established by compound **8** and the hMAO residues as described in the Experimental Section.

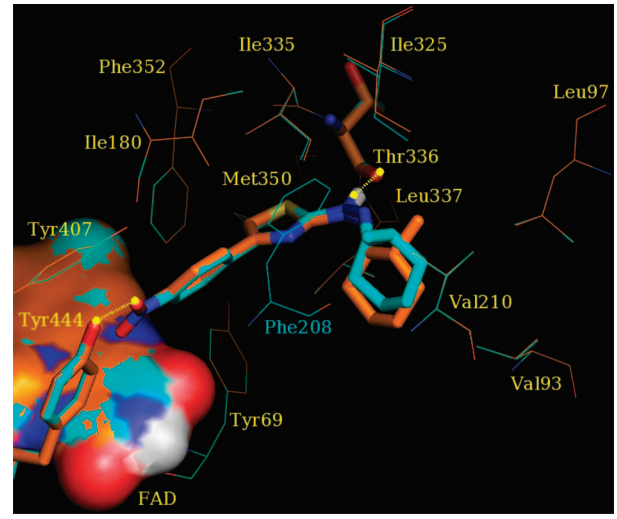

Figure 5. Superimposition of best fully energy minimized hMAO-A poses of (*R*)-**8** and (*S*)-**8** on protein Cα atoms. The ligand is depicted as orange carbon and light-blue carbon polytube models, respectively. The FAD cofactor is displayed with surface color coded carbons. The interacting residues with (*R*)-**8** and (*S*)-**8** are reported as orange and light-blue carbon wires, respectively. Hydrogen atoms are omitted for clarity, with the exception of the amminic one of **8**. Hydrogen bonds are reported as dotted lines. MAO residues establishing hydrogen bonds with **8** are rendered as polytubes.

In hMAO-A (Figure 5) **8** enantiomers showed a similar recognition pattern. In both cases the ligand established two hydrogen bonds. One was between the nitro group as acceptor and the phenolic hydroxyl moiety of Tyr444 as donor, the other was between the amine hydrogen as donor and the hydroxyl oxygen of Thr336 as acceptor. In the superimposition of these two complexes, which were carried out on the Cα atoms of the enzyme, the aromatic and the thiazole moieties of the enantiomers fit each other almost perfectly Conversely, the methyl moiety on the asymmetric carbon of the six-membered ring takes a different position within the cleft. The main consequence of this was that an additional hydrophobic contact of (*S*)-**8** was established with Phe208. This justifies the slightly better recognition of this enantiomer compared to (*R*)-**8**, as demonstrated by the interaction energies in agreement with the experimental inhibition data (Table 3). (*R*)-**8** and (*S*)-**8** respectively established 28 and 32 contacts with 13 and 14 residues of hMAO-A, as shown in Figure 5.

In MAO-B (Figure 6) the molecular recognition of (*R*)-**8** and (*S*)-**8** was significantly different. Even when the aromatic and the thiazole moieties were located approximately in the same area, i.e., close to the FAD, the fit between them was not perfect. The reason for this could be the different configuration of the C=N double bond, *Z* in (*R*)-**8** and *E* in

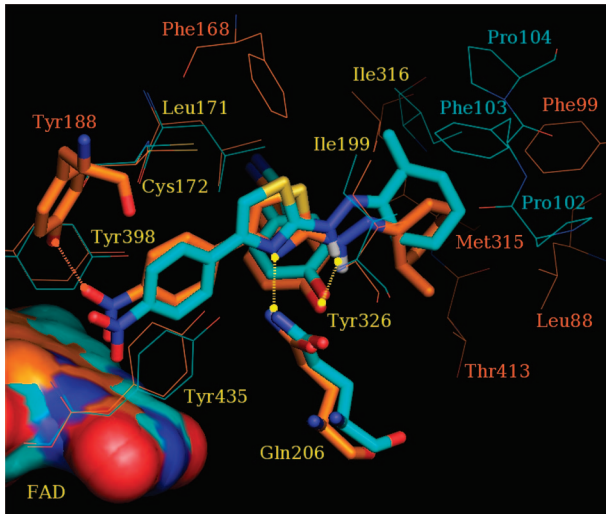

Figure 6. Superimposition of best fully energy minimized hMAO-B poses of (*R*)-**8** and (*S*)-**8** on protein Cα atoms. The ligand is depicted as orange carbon and light-blue carbon polytube models, respectively. The FAD cofactor is displayed with surface color coded carbons. The interacting residues with (*R*)-**8** and (*S*)-**8** are reported as orange and light-blue carbon wires, respectively, and common interacting residues are labeled yellow. Hydrogen atoms are omitted for clarity, with the exception of the amminic one of **8**. Common hydrogen bonds are reported as yellow dotted lines, the one specific for the (*R*)-**8**, orange. MAO residues establishing hydrogen bonds with **8** are rendered as polytubes.

(*S*)-**8**, best poses in the hMAO-B isoform. The interaction pattern is actually different also in terms of intermolecular hydrogen bonds. Two common hydrogen bonds were formed. One was between the thiazole nitrogen as acceptor and the amide hydrogen of the Gln206 side chain as donor, and the other was between the amine hydrogen as donor and the hydroxyl oxygen of Tyr326 as acceptor. For the (*R*)-**8** hMAO-B complex an additional hydrogen bond was also detected between the nitro group as donor and the hydroxyl oxygen of Tyr188 as acceptor. This additional H-bond, found in the (*R*)-**8** compound *Z* configuration, can explain the larger experimental inhibition difference of stereoisomers **8** onto the hMAO-B isoform versus the hMAO-A (Table 4). In terms of contacts and residues involved in hMAO-B recognition, an analysis of the most stable complexes revealed consistent differences. (*R*)-**8** and (*S*)-**8** respectively established 37 and 34 contacts with 13 and 11 residues of hMAO-B as shown in Figure 6. In this case the common contact residues are only eight, confirming a more consistent diversity in enantioselective recognition in the hMAO-B isoform compared to the hMAO-A. Another important consideration in the analysis of the isoform binding poses can be a double stacking of the nitrobenzene moiety with the Tyr398 and Tyr435 side chains (Figure 6). This is supposed to be a crucial interaction in the recognition of hMAO inhibitors. Since in hMAO-A the corresponding stacking with Tyr407 and Tyr444 was prevented by the hydrogen bond with the nitro group of **8** (Figure 5), the selectivity for the hMAO-B isoform can also be explained by the fact that the partial double $\pi-\pi$ interaction is missing.

In order to better explore the flexibility of the optimized docking configurations, the best poses were submitted to molecular dynamics experiments. The analysis of the results confirmed that the configurations obtained in both MAO isoforms with the stereoisomes of **8** were stable. The root-mean-square deviation (rmsd) with respect to the starting ligand geometry revealed fluctuations lower than 1.5 and 0.6 Å within the MAO A and B isoforms, respectively (see Supporting Information). This result suggests that our ligands are more favored to assume the bioactive conformations found within the MAO-B isoform than that within the A one. In agreement with the experimental selectivity inhibition our ligands appear to be conformationally preorganized to fit into the MAO-B gorge with a low entopic cost.

In conclusion, the molecular modeling study of the most active and selective hMAO inhibitor **8** was qualitatively in agreement with the selectivity for isoform B as well as the different enantioselective inhibition of the enantiomers for the same enzyme. Moreover, both MM and QM studies indicated that both *E* and *Z* configurations are thermodynamically possible for the inhibitor **8**. The docking results show that the *Z* configuration has the best recognition for hMAO-B. This information should be taken into account in the rational design of new more potent and selective inhibitors.

Experimental Section

Chemistry. General Procedure for the Preparation of 2-MCET and 2-Thiazolylhydrazone Derivatives (1−9). 2-Methylcyclohexanone (50 mmol) was dissolved in 100 mL of 2-propanol and refluxed under magnetic stirring with an equimolar amount of thiosemicarbazide for 24 h. The thiosemicarbazone 2-MCET precipitated from the reaction mixture, was filtered, and was crystallized from EtOH/CH_2Cl_2. The chemical and physical properties are reported in the Supporting Information.

Equimolar amounts of 2-MCET and bromoacetophenone, both dissolved in 2-propanol, were reacted at room temperature under stirring for 2 h. The white precipitate was filtered and crystallized from ethanol or ethanol/isopropanol to give compounds **1−9**. For compounds **1−9** we report the chemical and physical properties (see Supporting Information).

Pharmacological Studies: Determination of hMAO Isoforms Inhibitory Activity. The potential effects of the test drugs on hMAO activity were investigated by measuring their effects on the production of hydrogen peroxide from *p*-tyramine (a common substrate for both hMAO-A and hMAO-B), using the Amplex Red MAO assay kit (Molecular Probes, Inc., Eugene, OR) and microsomal MAO isoforms prepared from insect cells (BTI-TN-5B1-4) infected with recombinant baculovirus containing cDNA inserts for hMAO-A or hMAO-B (Sigma-Aldrich Química S.A., Alcobendas, Spain).

The production of H_2O_2 catalyzed by hMAO isoforms can be detected using 10-acetyl-3,7-dihydroxyphenoxazine (Amplex Red reagent), a nonfluorescent, highly sensitive, and stable probe that reacts with H_2O_2 in the presence of horseradish peroxidase to produce a fluorescent product: resorufin. In this study hMAO activity was evaluated using the above method following the general procedure described previously by us.[25]

Briefly, 0.1 mL of sodium phosphate buffer (0.05 M, pH 7.4) containing various concentrations of the test drugs (new compounds or reference inhibitors) and adequate amounts of the recombinant hMAO-A or hMAO-B were adjusted to obtain in our experimental conditions the same rection velocity, i.e., to oxidize (in the control group) the same concentration of substrate: 165 pmol of *p*-tyramine/min (hMAO-A, 1.1 μg; specific activity, 150 (nmol of *p*-tyramine oxidized to *p*-hydroxyphenylacetaldehyde/min)/mg protein; hMAO-B, 7.5 μg; specific activity, 22 (nmol of *p*-tyramine transformed/min)/mg protein) was incubated for 15 min at 37 °C in a flat-black-bottom 96-well microtiter (Microtest plate, BD, Franklin Lakes, NJ) placed in the dark fluorimeter chamber. After this incubation period, the reaction was started by adding (final concentrations) 200 μM Amplex Red reagent, 1 U/mL horseradish peroxidase, and 1 mM *p*-tyramine. The production of H_2O_2 and, consequently, of resorufin was quantified at 37 °C in a multidetection microplate fluorescence reader (FLX800, Bio-Tek Instruments, Inc., Winooski, VT) based on the fluorescence generated (excitation, 545 nm;

emission, 590 nm) over a 15 min period in which the fluorescence increased linearly.

Control experiments were carried out simultaneously by replacing the test drugs (new compounds and reference inhibitors) with appropriate dilutions of the vehicles. In addition, the possible capacity of the above test drugs to modify the fluorescence generated in the reaction mixture due to nonenzymatic inhibition (e.g., for directly reacting with Amplex Red reagent) was determined by adding these drugs to solutions containing only the Amplex Red reagent in a sodium phosphate buffer.

To determine the kinetic parameters of hMAO-A and hMAO-B (K_m and V_{max}), the corresponding enzymatic activity of both isoforms was evaluated (under the experimental conditions described above) in the presence of a number (a wide range) of *p*-tyramine concentrations.

The specific fluorescence emission (used to obtain the final results) was calculated after subtraction of the background activity, which was determined from vials containing all components except the MAO isoforms, which were replaced by a sodium phosphate buffer solution.

The corresponding IC_{50} values and MAO-B selectivity ratios [IC_{50}(MAO-A)]/[IC_{50}(MAO-B)] for the inhibitory effects of test drugs (new compounds and reference inhibitors) are shown in Tables 1 and 2.

Reversibility and Irreversibility Experiments. To evaluate whether the test compounds are reversible or irreversible MAO inhibitors, an effective centrifugation−ultrafiltration method (so-called repeated washing) was used. Briefly, adequate amounts of the recombinant hMAO-A or hMAO-B were incubated together with a single concentration (see Table 3) of the test drugs [racemic mixture and enantiomers of compound **5** and **8** and the reference inhibitors moclobemide and *R*-(−)-deprenyl in a sodium phosphate buffer (0.05 M, pH 7.4)] for 15 min at 37 °C. After this incubation period, an aliquot of this incubated sample was stored at 4 °C and used for subsequent measurement of MAO inhibitory activity under the experimental conditions indicated above (see the subsection on determination of MAO inhibitory activity). The remaining incubated sample (300 μL) was placed in a Ultrafree-0.5 centrifugal tube (Millipore, Billerica, MA) with a 30 kDa Biomax membrane in the middle of the tube and centrifuged (9000*g*, 20 min, 4 °C) in a centrifuge (J2-MI, Beckman Instruments, Inc., Palo Alto, CA). The enzyme retained in the 30 KDa membrane was resuspended in sodium phosphate buffer at 4 °C and centrifuged again (under the same experimental conditions described above) two successive times. After the third centrifugation, the enzyme retained in the membrane was resuspended in sodium phosphate buffer (300 μL) and an aliquot of this suspension was used for subsequent MAO activity determination.

Control experiments were performed simultaneously (to define 100% MAO activity) by replacing the test drugs with appropriate dilutions of the vehicles. The corresponding values of percent (%) MAO isoform inhibition were separately calculated for samples with and without repeated washing.

X-Ray Crystal Structure Analysis. (+)-2-MCET crystallizes from a solution of dichloromethane and ethanol as colorless needles. Crystal data: $C_{16}H_{30}N_6S_2$, $M = 370.58$, orthorhombic, space group $P212121$, $a = 8.194(1)$ Å, $b = 13.053(1)$ Å, $c = 19.254(1)$ Å, $V = 2059.3(3)$ Å^3, $Z = 4$, $D_c = 1.195$, $\mu = 2.416$ mm^{-1}, $F(000) = 800$.

Chromatographic (HPLC) Resolution of Racemic Samples 1−9. HPLC enantioseparations were performed using stainless-steel Chiralpak AD (250 mm × 4.6 mm i.d. and 250 mm × 10 mm i.d.) and Chiralpak AS-H (250 mm × 4.6 mm i.d. and 250 mm × 10 mm i.d.) (Daicel, Chemical Industries, Tokyo, Japan) columns. HPLC-grade solvents were supplied by Carlo Erba (Milan, Italy). The HPLC apparatus consisted of a Perkin-Elmer (Norwalk, CT) 200 lc pump equipped with a Rheodyne (Cotati, CA) injector, a HPLC Dionex (CA) model TCC-100 oven, and a Jasco (Jasco, Ishikawa-cho, Hachioji City, Tokyo, Japan) model 2095 Plus UV/CD detector.

The mobile phases were filtered and degassed by sonication immediately before. After the semipreparative separation, the collected fractions were analyzed on chiral analytical columns to determine their enantiomeric excess.

Molecular Modeling. The computational work was carried out in three steps considering the most active and selective compound **8** with a similar approach reported in our previous communication.[21]

All calculations were carried out with a Linux cluster of 16 Intel Xeon dual processors at 3.2 GHz with 2 Gb of RAM. Graphic manipulations and analysis of the docking experiments were performed with the Maestro Graphical User Interface, version 4.1.012, for Linux operating systems.[26] Ligplot, version 4.0,[27] and Pymol, version 0.98,[28] were used to create Figures 5 and 6.

The first step was the conformational analysis of **8**, which is complicated by the presence of the asymmetric methylcyclohexylidene moiety and the configuration of the thiosemicarbazone imine N=C double bond. Two Monte Carlo (MC) simulations were carried out using the (*R*)-enantiomer built in the *E* and *Z* configurations. Five-thousand conformations were randomly generated and energy-minimized with the MMFF force field in GB/SA water as implemented in the Macromodel package.[29] The conformational deduplication criterion was set as default, i.e., with a cutoff of 1 kcal/mol and an rms threshold of 0.25 Å.

The *E* and *Z* global minimum conformers were both submitted to an ab initio single point DFT-B3LYP energy calculation with Jaguar,[26] at 6-311G**++ basis set in three different environments: vacuum, water, and 1,2-dichloroethane.

The mirror images of the (*S*)-*E* and (*S*)-*Z* stereoisomers were respectively obtained by inverting the sign of the *Z* atomic coordinates of the (*R*)-*E* and (*R*)-*Z* conformers of **8** obtained in the MC search using the MOLINE conversion module.[30]

The second step of the modeling work was the pretreatment of the hMAO enzyme crystallographic models. Following computational work in our recent communications,[31] the Protein Data Bank[32] crystallographic models of hMAO-A and hMAO-B, respectively known by the PDB codes 2BXR[17] and 1GOS,[16] were used for the docking experiments. Both structures were obtained as adducts with two similar compounds, clorgyline for 2BXR and pargyline for 1GOS, covalently linked to the FAD N5 nitrogen.

After removal of the covalent bond between the FAD moiety and the cocrystallized inhibitor, pretreatment of the original PDB models consisted of a 48 kcal/mol constrained energy minimization of those residues out of a radius of 15 Å from N5 of the isoalloxazine ring in order to restore the natural planarity of the isoalloxazine FAD ring and relax the active site amino acids. The resulting energy minimum structure ligands were removed and used as receptor models. This was done with the AMBER* force field united atom notation and the GB/SA water model of solvation as implemented in MacroModel.[26]

The third step was the docking into the hMAO receptor models. All energy minimum conformers of the four **8** stereoisomers were docked in the hMAO binding sites with the GLIDE docking method.[33] Both pretreated enzyme models were submitted to map calculations using a box of about 110 000 Å^3 centered on the FAD N5 atom. The rigid docking of the **8** stereoisomers was done by generating a maximum number of 5000 configurations, scaling the ligand van der Waals radii by 50%. All complex configurations were fully energy-minimized with the AMBER* united atom and the GB/SA water model of solvation.[26]

After full relaxation, the interaction energy of all complexes was computed according to the MOLINE method[30] and compared to the experimental inhibition data.

In order to highlight the hMAO residues involved in van der Waals and hydrogen bonds in the recognition of **8** in the enzyme, the most stable fully energy-minimized configurations (Table 4) of four complexes [(*R*)-**8**·hMAO-A], [(*S*)-**8**·hMAO-A], [(*R*)-**8**·hMAO-B], and [(*S*)-**8**·hMAO-B] were analyzed using the LigPlot program.[27]

Acknowledgment. This work was supported by grants from MURST (Italy), Ministerio de Sanidad y Consumo (Spain,

Grant FISS PI061537), and Xunta de Galicia (Spain, Grant PGIDIT05BTF20302PR). We acknowledge Anton Gerada, a professional translator, Fellow of the Institute of Translation and Interpreting of London and Member of AIIC (Association Internationale des Interprêtes de Conférences, Geneva), for the revision of the manuscript. We acknowledge Dott. Cristina Faggi of the Department of Organic Chemistry of the University of Florence for the X-ray structure analysis. F.O. especially grateful to the Consellería de Educación e Ordenación Universitaria de la Xunta de Galicia (Spain) for giving him financial support to intensify his research activity and to reduce his teaching during the academic year 2007−2008 [programa de promoción de intensificación de la actividad investigadora en el sistema Universitario de Galicia (SUG)].

Supporting Information Available: Analytical and spectral data for new compounds, chromatography conditions, X-ray data, computational data, and a few details on pharmacological studies. This material is available free of charge via the Internet at http://pubs.acs.org.

References

(1) Edmondson, D. E.; Mattevi, A.; Binda, C.; Li, M.; Hubálek, F. Structure and mechanism of monoamine oxidase. *Curr. Med. Chem.* **2004**, *11*, 1983–1993.
(2) Shih, J. C.; Chen, K. Regulation of MAO-A and MAO-B gene expression. *Curr. Med. Chem.* **2004**, *11*, 1995–2005.
(3) Shih, J. C.; Chen, K.; Ridd, M. J. Monoamine oxidase: from genes to behavior. *Annu. Rev. Neurosci.* **1999**, *22*, 197–217.
(4) Weyler, W.; Hsu, Y. P.; Breakefield, X. O. Biochemistry and genetics of monoamine oxidase. *Pharmacol. Ther.* **1990**, *47*, 391–417.
(5) Da Prada, M.; Kettler, R.; Keller, H. H.; Cesura, A. M.; Richards, J. G.; Saura Marti, J.; Muggli-Maniglio, D.; Wyss, P. C.; Kyburz, E.; Imhof, R. From moclobemide to Ro 19-6327 and Ro 41-1049: the development of a new class of reversible, selective MAO-A and MAO-B inhibitors. *J. Neural. Transm., Suppl.* **1990**, *29*, 279–292.
(6) Guay, D. R. Rasagiline (TVP-1012): a new selective monoamine oxidase inhibitor for Parkinson's disease. *Am. J. Geriatr. Pharmacother.* **2006**, *4* (4), 330–346.
(7) Shih, J. C. Cloning, after cloning, knock-out mice and physiological functions of MAO A and B. *Neurotoxicology* **2004**, *25*, 21–30.
(8) Riederer, P.; Lachenmayer, L.; Laux, G. Clinical applications of MAO-inhibitors. *Curr. Med. Chem.* **2004**, *11*, 2033–2043.
(9) Strolin-Benedetti, M.; Dostert, P. L. Monoamine oxidase: from physiology and pathophysiology to the design and clinical application of reversible inhibitors. *Adv. Drug Res.* **1992**, *23*, 65–125.
(10) Wouters, J. Structural aspects of monoamine oxidase and its reversible inhibition. *Curr. Med. Chem* **1998**, *5* (2), 137–162.
(11) Cash, A. D.; Perry, G.; Smith, M. A. Therapeutic potential in Alzheimer's disease. *Curr. Med. Chem* **2002**, *9* (17), 1605–1610.
(12) Carreiras, M. C.; Marco, J. L. Recent approaches to novel anti-Alzheimer therapy. *Curr. Pharm. Des.* **2004**, *10* (25), 3167–3175.
(13) Drukarch, B.; Muiswinkel, F. L. Drug treatment of Parkinson's disease. *Biochem. Pharmacol.* **2000**, *59*, 1023–1031.
(14) Pacher, P.; Kohegyi, E.; Kecskemeti, V.; Furst, S. Current trends in the development of new antidepressants. *Curr. Med. Chem.* **2001**, *8* (2), 89–100.
(15) Pacher, P.; Kecskemeti, V. Trends in the development of new antidepressants. Is there a light at the end of the tunnel? *Curr. Med. Chem.* **2004**, *11* (7), 925–943.
(16) Binda, C.; Newton-Vinson, P.; Hubálek, F.; Edmondson, D. E.; Mattevi, A. Structure of human monoamine oxidase B, a drug target for the treatment of neurological disorders. *Nat. Struct. Biol.* **2002**, *9*, 22–26. (data deposition: www.pdb.org (PDB ID code 1GOS)
(17) De Colibus, L.; Li, M.; Binda, C.; Lustig, A.; Edmondson, D. E.; Mattevi, A. Three-dimensional structure of human monoamine oxidase A (MAO A): relation to the structures of rat MAO A and human MAO B. *Proc. Natl. Acad. Sci. U.S.A.* **2005**, *102* (36), 12684–12689. (data deposition: www.pdb.org (PDB ID codes 2BXR, 2BXS, and 2BYB)
(18) Binda, C.; Hubálek, F.; Li, M.; Edmondson, D. E.; Mattevi, A. Crystal structure of human monoamine oxidase B, a drug target enzyme monotopically inserted into the mitochondrial outer membrane. *FEBS Lett.* **2004**, *564* (3), 225–228.
(19) Binda, C.; Edmondson, D. E.; Mattevi, A. Structure−function relationships in flavoenzyme-dependent amine oxidations. A comparison of polyamine oxidase and monoamine oxidase. *J. Biol. Chem.* **2002**, *277* (27), 23973–23976.
(20) Hubálek, F.; Binda, C.; Khalil, A.; Li, M.; Mattevi, A.; Castagnoli, N.; Edmondson, D. E. Demonstration of isoleucine 199 as a structural determinant for the selective inhibition of human monoamine oxidase B by specific reversible inhibitors. *J. Biol. Chem.* **2005**, *280* (16), 15761–15766.
(21) Chimenti, F.; Maccioni, E.; Secci, D.; Bolasco, A.; Chimenti, P.; Granese, A.; Befani, O.; Turini, P.; Alcaro, S.; Ortuso, F.; Cardia, M. C.; Distinto, S. Selective inhibitory activity against MAO and molecular modeling studies of 2-thiazolylhydrazone derivatives. *J. Med. Chem.* **2007**, *50*, 707–712.
(22) Maccioni, E.; Cardia, M. C.; Bonsignore, L.; Plumitallo, A.; Pellerano, M. L.; DeLogu, A. Synthesis and anti-microbial activity of isothiosemicarbazones and cyclic analogues. *Farmaco* **2002**, *57* (10), 809–817.
(23) Maccioni, E.; Cardia, M. C.; Distinto, S.; Bonsignore, L.; De.Logu, A. An investigation of the biological effect of structural modifications of isothiosemicarbazones and their cyclic analogues. *Farmaco* **2003**, *58* (9), 951–959.
(24) Cirilli, R.; Ferretti, R.; La Torre, F.; Secci, D.; Bolasco, A.; Carradori, S.; Pierini, M. High-performance liquid chromatographic separation of enantiomers and diastereomers of 2-methylcyclohexanone thiosemicarbazone, and determination of absolute configuration and configurational stability. *J. Chromatogr., A* **2007**, *1172*, 160–169.
(25) Yáñez, M.; Fraiz, N.; Cano, E.; Orallo, F. Inhibitory effects of *cis*- and *trans*-resveratrol on noradrenaline and 5-hydroxytryptamine uptake and on monoamine oxidase activity. *Biochem. Biophys. Res. Commun.* **2006**, *344*, 688–695.
(26) *MacroModel*, version 7.2; Schrödinger Inc.: Portland, OR, 1998−2001.
(27) Wallace, A. C.; Laskowski, R. A.; Thornton, J. LIGPLOT: a program to generate schematic diagrams of protein−ligand interactions. *Protein Eng.* **1995**, *8*, 127–134.
(28) DeLano, W. L. *The PyMOL Molecular Graphics System*; DeLano Scientific: San Carlos, CA, 2002; http://www.pymol.org.
(29) *Jaguar*, version 4.1; Schrödinger Inc.: Portland, OR, 1998−2001.
(30) Alcaro, S.; Gasparrini, F.; Incani, O.; Caglioti, L.; Pierini, M.; Villani, C. A quasi flexible automatic docking processing for studying stereoselective recognition mechanisms. Part II. Prediction of $\Delta\Delta G$ of complexation and ^{1}H-NMR NOE. *J. Comput. Chem.* **2007**, *28*, 1119–1128.
(31) (a) Chimenti, F.; Maccioni, E.; Secci, D.; Bolasco, A.; Chimenti, P.; Granese, A.; Befani, O.; Turini, P.; Alcaro, S.; Ortuso, F.; Cirilli, R.; La.Torre, F.; Cardia, M. C.; Distinto, S. Synthesis, molecular modeling studies and selective inhibitory activity against MAO of 1-thiocarbamoyl-3,5-diaryl-4,5-dihydro-(1*H*)-pyrazole derivatives. *J. Med. Chem.* **2005**, *48*, 7113–7122. (b) Chimenti, F.; Bolasco, A.; Manna, F.; Secci, D.; Chimenti, P.; Granese, A.; Befani, O.; Turini, P.; Alcaro, S.; Ortuso, F. Synthesis and molecular modelling of novel substituted-4,5-dihydro-(1*H*)-pyrazole derivatives as potent and highly selective monoamine oxidase-A inhibitors. *Chem. Biol. Drug Des.* **2006**, *67*, 206–214. (c) Chimenti, F.; Bolasco, A.; Manna, F.; Secci, D.; Chimenti, P.; Granese, A.; Befani, O.; Turini, P.; Cirilli, R.; La.Torre, F.; Alcaro, S.; Ortuso, F.; Langer, T. Synthesis, biological evaluation and 3D-QSAR of 1,3,5-trisubstituted-4,5-dihydro-(1*H*)-pyrazole derivatives as potent and highly selective monoamine oxidase A inhibitors. *Curr. Med. Chem.* **2006**, *13*, 1411–1428.
(32) Berman, H. M.; Westbrook, J.; Feng, Z.; Gilliland, G.; Bhat, T. N.; Weissig, H.; Shindyalov, I. N.; Bourne, P. E. The Protein Data Bank. *Nucleic Acids Res.* **2000**, *28*, 235–242.
(33) Eldridge, M. D.; Murray, C. W.; Auton, T. R.; Paolini, G. V.; Mee, R. P. Empirical scoring functions: 1. The development of a fast empirical scoring function to estimate the binding affinity of ligands in receptor complexes. *J. Comput.-Aided Mol. Des.* **1997**, *11*, 425–445.

JM800132G